

Infrared activity of hydrogen molecules trapped in Si

B. Hourahine and R. Jones

School of Physics, The University of Exeter, Exeter EX4 4QL, United Kingdom

(Received 27 January 2003; published 19 March 2003)

The rovibrational-translational states of a hydrogen molecule moving in a cage site in Si, when subjected to an electrical field arising from its surroundings, are investigated. The wave functions are expressed in terms of basis functions consisting of the eigenfunctions of the molecule confined to move in the cavity and rovibrational states of the free molecule. The energy levels, intensities of infrared and Raman transitions, effects of uniaxial stress, and a neighboring oxygen defect are found and compared with existing experimental data.

DOI: 10.1103/PhysRevB.67.121205

PACS number(s): 61.72.Bb, 71.55.-i, 85.40.Ry

Hydrogen molecules have long been expected to be low-energy defects in Si,^{1,2} but the observation by infrared (IR) absorption of what appeared to be isolated hydrogen molecules trapped at cage sites was quite unexpected.^{3,4} While there is no difficulty in understanding that molecules trapped at low-symmetry sites in a range of materials^{6,7} would be IR active, the same is not true with molecules at tetrahedral cage sites in Si. The usual argument to explain their activity is that the lattice electric field F_i induces a dipole moment $\alpha_{ij}F_j$ on the molecule in direction i .⁵ Here, α_{ij} is the molecular polarizability. However, the electric field at the T_d cage site is actually zero, and a zero-point movement of the center of mass of the molecule has been invoked to provide an interaction.^{8,9} Now, if the molecule can freely rotate, Condon noted¹⁰ that this dipole moment couples with the electric field of the IR radiation and leads to the same selection rules as for Raman scattering: namely, $\Delta j=0$ or 2. In addition, transitions involving both ortho- H_2 with $j=1$, and para- H_2 with $j=0$, should occur and hence *four* IR transitions¹¹ are expected at low temperatures. However, experiments⁴ indicate that only one mode at 3618.4 cm^{-1} is detected. This has led to suggestions that the molecule is static but recent studies^{9,12} demonstrate that this is not correct and the mode arises from a $\Delta j=0$ transition from a degenerate $j=1$ state. Thus it appears that the para- H_2 species is not IR active – possibly because of symmetry reasons.¹² A further difficulty then emerges when considering the transitions for HD. Two transitions are detected⁹ corresponding to $\Delta j=1$ and $\Delta j=0$. The first disagrees with Condon's analysis and implies that something new is needed.

We show here, using a simple model, that the infrared intensity does not arise from the polarization induced in the molecule undergoing zero-point motion, but from a polarization of the Si lattice by the electric field arising from the quadrupole moment of a rotating molecule. Further, we show that the ground state of the para- H_2 species transforms as A_1 and the only dipole allowed transition involves a so far undetected $\Delta j=2$ transition. Transitions between T_2 states accounts for the observed $\Delta j=0$ transition. The effect of a *nonuniform* electric field due to the lattice on the molecule is crucially important in understanding the activity of HD. We show that two transitions with $\Delta j=0$ and 1 then arise. Moreover, the model accounts for the effect of stress and a nearby oxygen impurity on the molecular spectrum.

The Hamiltonian of the molecule moving in the cage surrounding a tetrahedral site contains kinetic and potential

terms dependent on the center-of-mass coordinates, defined by spherical polar coordinates (R, Θ, Φ) , as well as internal coordinates defined by the molecular length and orientation in space (r, θ, ϕ) with the axes assumed parallel to the cube edges. For a spherical cavity, the translational motion leads to a center-of-mass wave function described by $f_L(R)Y_{LM}(\Theta, \Phi)$, and the internal motion to rovibrational wave functions $\chi_\nu(r-r_e)Y_{jm}(\theta, \phi)$. For illustrative purposes, we take $f_L(R)$ to be a δ function so that the center of mass is at a fixed distance, $R \sim 0.13\text{ \AA}$, from the T_d site: a value consistent with the zero-point displacement found by molecular dynamics.¹³ Our results are, however, insensitive to R . The electric field F_i arising from the lattice is modeled by placing charges of $4e$ on each Si atom and $-2e$ at each bond center and, where relevant, an additional $-e/9$ at a bond centered oxygen interstitial. Such a field is at the upper limit of what is to be expected. We have assumed that there is no charge density at the T_d site. In fact, this leads to a reduction in the vibration frequency of the molecule which we can take into account by reducing the molecular stretch force constant.¹⁴ The potential energy of the molecule depends on the electric field F_i and its gradient $F_{i,j}$ at the center of the molecule and is given by^{6,7}

$$-\frac{1}{2}\alpha_{ij}F_iF_j - \frac{1}{3}\Theta_{ij}F_{i,j},$$

where the polarizability and quadrupole moment are expressed in terms of the molecule alignment \mathbf{r} by

$$\alpha_{ij} = \alpha(r)\delta_{ij} + \frac{\gamma(r)}{3r^2}(3r_i r_j - r^2\delta_{ij}), \quad (1)$$

$$\Theta_{ij} = \frac{1}{2r^2}\Theta(r)(3r_i r_j - r^2\delta_{ij}).$$

This energy depends on both the position of the center of mass and the molecular alignment. Figure 1 shows this molecular potential energy, which is dominated by the quadrupole term, of the H_2 molecule when the center of mass is located at (R, Θ, Φ) , with $R=0.13\text{ \AA}$, while aligned along $\theta=\Theta, \phi=\Phi$ with r equal to the equilibrium bond length r_e . We note that variations in the potential are $\sim \pm 200\text{ cm}^{-1}$ and directions where the molecule is aligned away from the four Si neighbors are favored. The weak potential is consistent with *ab initio* calculations¹⁵ and would not prevent molecular rotation.¹⁶ This justifies our use of basis states made from those of a freely rotating molecule. The Hamiltonian

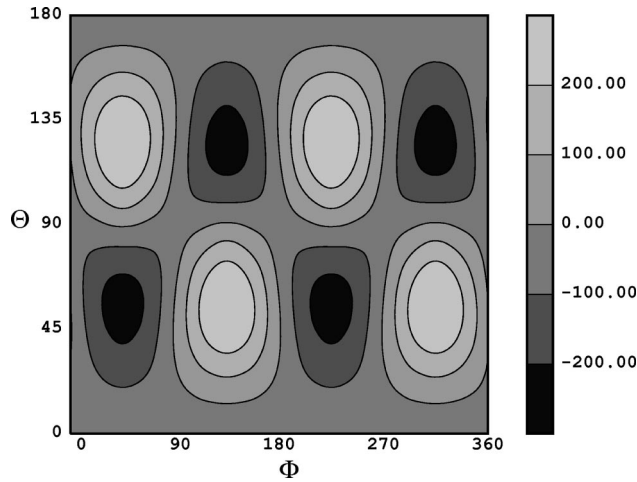


FIG. 1. Potential energy (per centimeter) of the H_2 molecule at (R, Θ, Φ) with $R=0.13 \text{ \AA}$ and aligned along (Θ, Φ) . The directions to the four Si neighbors correspond to $\Theta=54.5^\circ, \Phi=135^\circ$ and 315° , $\Theta=125.3^\circ, \Phi=45^\circ$ and 225° , and to peaks in the potential.

matrix elements for each vibrational state ν , in the absence of F_i , are $\hbar\omega_0(\nu+1/2) + B_\nu j(j+1)/\mu + 2L\Delta/M$. Here, ω_0, B_ν, μ , and M are the fundamental stretch frequency, rovibrational constant, reduced mass, and total molecular mass. $2\Delta/M$ is the energy separation between $L=0$ and $L=1$ cavity states that we take for H_2 to be $\sim 1000 \text{ cm}^{-1}$ which again can be related to the energy profile of the molecule around the T_d site.¹³ A Taylor series expansion of $\alpha(r), \gamma(r)$, and $\Theta(r)$ about r_e with the molecular constants taken from Refs. 7 and 17 enabled the potential-energy matrix elements to be found numerically using Lebedev's method. Matrix elements of this Hamiltonian between different rotational, $j < 6$, and cavity states, $L < 2$, were found for each ν and the energy levels and wave functions determined.

The intensity of an infrared transition between states $|\nu=0, n\rangle$ and $|\nu=1, m\rangle$ is related to the transition dipole moment $P_i(n, m)$ in direction i . This has two contributions: the first comes from the induced dipole, as given by Condon, and the second comes from the dipole induced in the Si lattice by the molecule. The second term is found from the field $F_i(a)$ arising from the quadrupole moment of the molecule at the site of an atom a with atomic polarizability α_a :²³

$$P_i(n, m) = \left\langle \nu=0, n \left| \alpha_{ij} F_j + \sum_a \alpha_a F_i(a) \right| \nu=1, m \right\rangle \\ \sim \sqrt{\frac{\hbar}{2\mu\omega_0}} \left\langle n \left| \left\{ \alpha'_{ij} F_j + \sum_a \alpha_a F'_i(a) \right\} \right| m \right\rangle, \quad (2)$$

where the prime denotes the derivative with r . The effective charge for the oscillator is $\sqrt{\{2\mu\omega_0 \sum'_{n,m} |P(n, m)|^2 / (3\hbar)\}}$,¹⁸ where the sum is over degenerate n and m states. The first term in P_i is zero when $R=0$ as then F_i vanishes and is of order $10^{-3}e$ for $R \sim 0.13 \text{ \AA}$. The second term dominates and

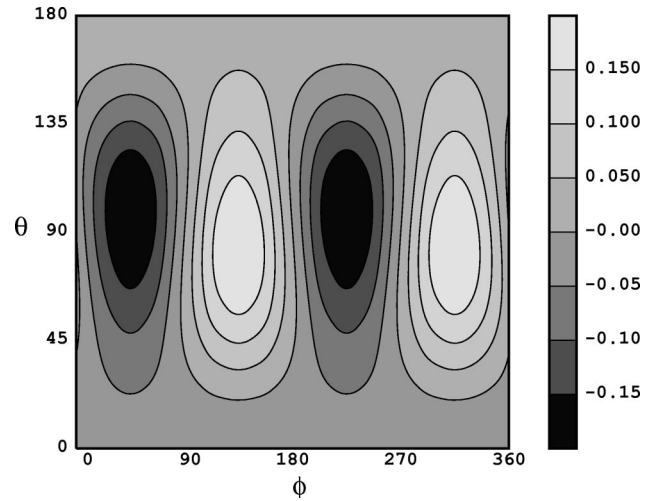


FIG. 2. z component of effective charge vector $\alpha'_{ij}(\theta, \phi) F_j + \sum_a \alpha_a F'_i(\theta, \phi, a)$, in units of e , of a H_2 molecule at the T_d site vs θ, ϕ describing its alignment. Note that the effective charge varies by $\pm 0.15e$.

Fig. 2 shows that its z component has a magnitude compatible with the experimental effective charge of $\sim 0.08e$.⁴ The strength of a Raman transition is proportional to $\sum'_{n,m,i,j} (\langle n | \alpha'_{ij} | m \rangle)^2$. Condon's result is easily derived from Eqs. (1) and (2) when F_i is a fixed uniform field.

Rotating H_2 by 180° about its center of mass leaves the Hamiltonian and dipole moment unchanged. This symmetry allows us to classify each state as "even," $+$, or "odd," $-$, corresponding to para- and ortho-hydrogen, respectively. For H_2 , the ground state has A_1^+ symmetry and is derived from orbitals with even j , while the first excited state has T_2^- symmetry and arises from orbitals with odd j . Both states have contributions from the $L=0$ and $L=1$ cavity orbitals. Figure 3 shows the ground-state wave function that is peaked in the troughs of the potential, i.e., in the direction away from the Si atoms.

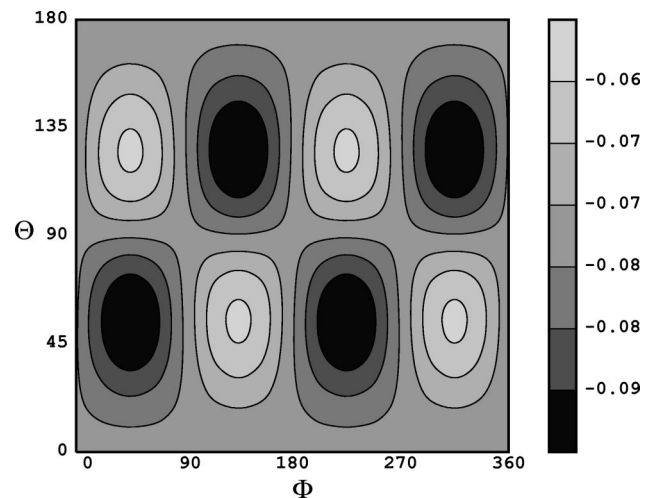


FIG. 3. A_1^+ wave function for center of mass of H_2 molecule at (R, Θ, Φ) , with $R=0.13 \text{ \AA}$, and aligned along (Θ, Φ) . Note that the peaks correspond with directions away from the four Si neighbors. The wave function is normalized over the surface of a sphere.

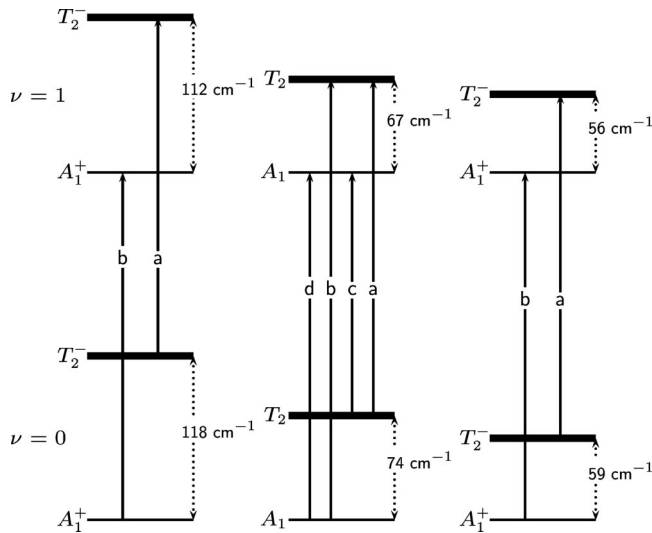


FIG. 4. Calculated rovibrational levels of (a) H_2 , (b) HD , and (c) D_2 at the T_d site in silicon. For H_2 and D_2 , only transitions a are IR active with effective charges of $0.1e$, while both a and b are Raman active with relative strengths of 3:1. For HD , transitions a , b , and c are all infrared active with effective charges of $0.12e$, $0.06e$ and $0.06e$. Only transitions a and d are Raman active with relative strengths of 3:1. The nuclear wave functions and degeneracy have not been included in the symmetry classification of the states or the transition strengths.

The dipole moment transforms as T_2^+ and hence an orbitally degenerate state *must* comprise the initial or final IR transition and parity must be conserved. Thus, as noted in Ref. 9, transitions between A_1^+ states are IR inactive, in contrast with transitions between T_2^- states of ortho-hydrogen. Figure 4 shows the lowest-energy states and their symmetries for $\nu=0$ and 1 along with the intensities of the IR and Raman-active transitions between them. An IR-active transition [not shown in Fig 4(a)] involving para- H_2 between A_1^+ and T_2^+ , derived primarily from a $j=2$ orbital, occurs $\sim 340 \text{ cm}^{-1}$ above the ortho-transition with an effective charge of $\sim 0.1e$, but this has not been detected. The only detected transition, labeled a in Fig 4(a), has a strength in good agreement with the calculation. Very recently, Raman scattering has detected the transition between A_1^+ states in both H_2 and D_2 .¹⁹

For HD on the other hand, rotating the molecule by 180° about its center of mass displaces the center of the molecule to a new location. Its interaction with the surrounding lattice is then changed, as the field F_i is nonuniform, and the Hamiltonian and dipole moment are now different. Parity is then *not* conserved and transitions between A_1 and T_2 states are now possible as shown in Fig. 4(b). At low temperatures, only the $A_1 \rightarrow T_2$ b transition is seen but the stronger transition between T_2 states, labeled a , is detected at $\geq 23 \text{ K}$ after molecules have been thermally excited from A_1 to T_2 . The experimental ratio of the effective charges for the a and b transitions is 2.6:1 compared with 2:1 found here. The weaker $T_2 \rightarrow A_1$ transition c has not been reported to date. The calculated $\nu=0, A_1-T_2$ separation of 74 cm^{-1} is in very good agreement with the experimental value of 71 cm^{-1} .

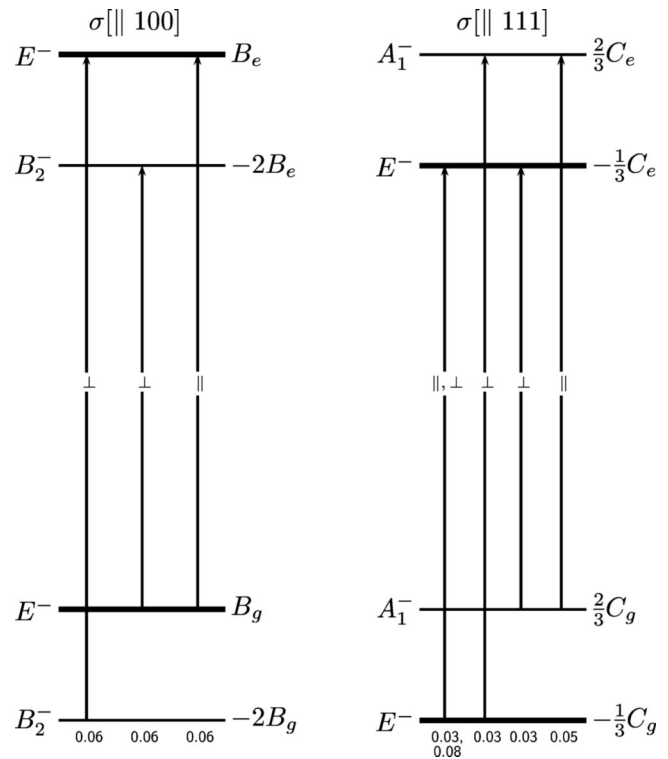


FIG. 5. The calculated splitting of the $T_2^- \rightarrow T_2^-$ transitions of H_2 at the T_d site for [100] and [111] applied stress. The effective charges of the split components are shown along with polarization selection rules.

Application of a general stress results in a displacement of the lattice and a change to the field F_i . The symmetry is now lowered leading to a splitting of the T_2^- levels. We take the atomic displacements to be given by elasticity theory and Fig. 5 shows the calculated splittings in the T_2^- manifolds for H_2 . We find the piezospectroscopic parameters B_g , C_g , B_e , and C_e (Fig. 5), respectively, to be 4.3, 5.4, 4.6, and $5.5 \text{ cm}^{-1} \text{ GPa}^{-1}$. These are in excellent agreement with experimental values of 4.5, 5.4, 4.5, and $5.4 \text{ cm}^{-1} \text{ GPa}^{-1}$ found by assuming identical shifts for $\nu=0$ and $\nu=1$. For D_2 , we get 4.1, 5.3, 4.2, and $5.9 \text{ cm}^{-1} \text{ GPa}^{-1}$ demonstrating that the splittings are almost independent of isotopic mass in agreement with earlier theoretical and experimental findings.¹² As has been noted previously, this result arises from the mass independence of the interaction given in Eq. (1).

The presence of oxygen at a neighboring bond center site leads to an additional electric field and a change in symmetry to C_{1h} , or to $C_{\infty h}$ if the lattice field is negligible. This also results in a splitting of the T_2 states and to a greater number of IR transitions. We assume that the perturbation by oxygen can be modeled by a single point charge, and neglect the strain due to the impurity, and show in Fig. 6 the spectra for H_2 , HD , and D_2 . Experimentally for H_2 , transitions a , b , and c are detected²⁰ in agreement with the calculations with the energy separations $c-b$ and $a-b$ being 6.1 and 57.9 cm^{-1} , respectively, compared with 10 and 68 cm^{-1} found here.

For HD , four transitions, h , b , a , and d are observed—two weak ones from the ground and two from the first excited

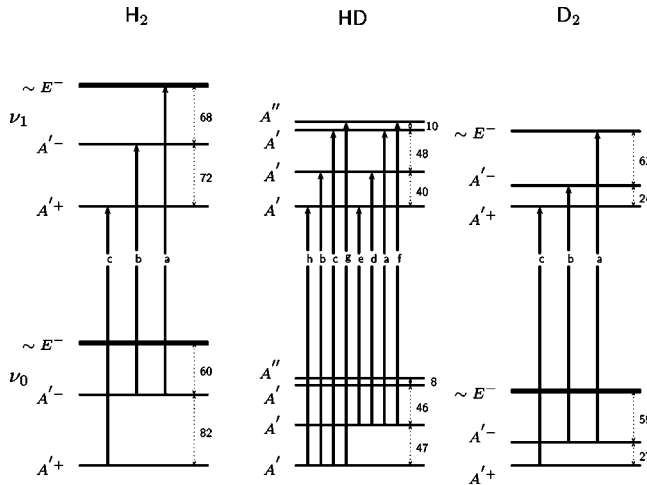


FIG. 6. Calculated rovibrational levels of H_2 , HD, and D_2 near O_{BC} . Only transitions arising from ground and first excited state are given. For H_2 and D_2 transitions $a-c$ are infrared active with effective charges of $0.10e$, $0.06e$, $0.02e$ and $0.10e$, $0.07e$, $0.03e$, respectively. Transitions b and c are also strongly Raman active with relative strengths 1:1. For HD, transitions $a-h$ are all infrared active with effective charges of $0.08e$, $0.06e$, $0.06e$, $0.06e$, $0.06e$, $0.05e$, $0.04e$, and $0.03e$. Only transitions b and d are strongly Raman active with equal strengths. The E state of HD is split by about 9 cm^{-1} .

state. We find that transitions $a-h$ are all active with transitions $b-e$ all being of similar activity. The energy separations and transition strengths found here for all the defects are not especially sensitive to the parameters R and Δ , but in the case of oxygen, they are sensitive to the assumed charge on oxygen and clearly the model will only obtain the correct transitions if this is modeled correctly. If the lattice polarization is reduced with respect to the charge on oxygen, then agreement is found with experiment in that only two dominant transitions h , b from the ground, and a , d from the first excited state, occur. The separation of b and h according to our theory is 40 cm^{-1} and about twice the observed value of

19 cm^{-1} but the separation between a and d is 48 cm^{-1} in fair agreement with experiment at 58.6 cm^{-1} . Much better agreement with the experimental ortho-para splitting has been found by a similar method but using a quite different perturbing potential.²¹

In conclusion, we have found that the IR activity of the molecule does not require a movement of the molecule away from the tetrahedral site, as has been thought previously, but a polarization of the surrounding lattice. The effective charges relating to the strengths of the IR transition are then the same for H_2 as D_2 and in agreement with the data, unlike a model where the activity arises from a displacement of the molecule from the lattice site.²¹ The splitting of the lines observed under stress, or by the presence of a neighboring oxygen impurity, can be modeled in a simple way and the results are in reasonable agreement with experiment. The analysis shows that there are other as yet undetected IR transitions at low temperatures albeit with low intensities. The method we have introduced is clearly applicable to molecules in a wide range of materials, e.g., GaN.

Finally, we note an interesting consequence of the splitting of the T_2^- state of H_2 in the presence of oxygen. The energy separation between the energetically lowest ortho- A'^- state and para- A'^+ states is only 82 cm^{-1} for H_2 near O, compared with 118 cm^{-1} for H_2 at a T_d site. This implies that ortho molecules would favor the former sites. It is known that H_2 is weakly bound to oxygen with a binding energy about 0.28 eV .²² Upon warming to around 30°C , molecules move reversibly between the two sites. Thus ortho- H_2 near oxygen sites is in equilibrium with the same nuclear species at T_d sites. This is also true for the para species. However, the binding energy of ortho- H_2 at O sites is lower by $118-82$ or 36 cm^{-1} than for para- H_2 . Thus, the equilibrium fraction of ortho- to para- H_2 species at oxygen sites should be about 20% larger than at T_d sites. Such an effect has not yet been reported.

We thank Ron Newman for many discussions during the course of this work.

¹A. Mainwood and A.M. Stoneham, *Physica B & C* **116**, 101 (1983).

²J.W. Corbett *et al.*, *Phys. Lett. A* **93**, 303 (1983).

³R.E. Pritchard *et al.*, *Phys. Rev. B* **56**, 13 118 (1997).

⁴R.E. Pritchard *et al.*, *Phys. Rev. B* **57**, 15 048 (1998).

⁵We use Einstein summation convention for repeated indexes

⁶J.D. Poll and J.L. Hunt, *Can. J. Phys.* **63**, 84 (1985).

⁷N. Bras, *J. Chem. Phys.* **110**, 5943 (1999).

⁸A.M. Stoneham, *Phys. Rev. Lett.* **84**, 4777 (2000).

⁹E.E. Chen *et al.*, *Phys. Rev. Lett.* **88**, 105507 (2002).

¹⁰E.U. Condon, *Phys. Rev.* **41**, 759 (1932).

¹¹This ignores splitting of the $j=2$ state into T_2+E .

¹²E.E. Chen *et al.*, *Phys. Rev. Lett.* **88**, 245503 (2002).

¹³S.K. Estreicher *et al.*, *J. Phys.: Condens. Matter* **13**, 6271 (2001).

¹⁴J.K. Nørskov, *Phys. Rev. B* **20**, 446 (1979).

¹⁵C.G. Van de Walle, *Phys. Rev. Lett.* **80**, 2177 (1998).

¹⁶B. Hourahine *et al.*, *Phys. Rev. B* **57**, 12 666 (1998).

¹⁷G. Herzberg, *Spectra of Diatomic Molecules*, 2nd ed. (Van Nostrand Reinhold, New York, 1950).

¹⁸B. Clerjaud and D. Côte, *J. Phys.: Condens. Matter* **4**, 9919 (1992).

¹⁹E.V. Lavrov and J. Weber, *Phys. Rev. Lett.* **89**, 215501 (2002).

²⁰E.E. Chen, M. Stavola, and W. Beall Fowler, *Phys. Rev. B* **65**, 245208 (2002).

²¹W. Beall Fowler, P. Walters, and M. Stavola, *Phys. Rev. B* **66**, 075216 (2002).

²²V.P. Markevich and M. Suezawa, *J. Appl. Phys.* **83**, 2988 (1998).

²³We take α to be 20 a.u. and related to the bulk Si dielectric constant by the Clausius-Mossotti relation $\alpha = (3/\epsilon_0) \times (\epsilon_r - 1)/(\epsilon_r + 2)$ (see Ref. 24).

²⁴I. Vasiliev, S. Ögüt, and J.R. Chelikowsky, *Phys. Rev. Lett.* **78**, 4805 (1997).